

# Dispersion of Surface Plasmon Polaritons on Metal Wires in the Terahertz Frequency Range

Kanglin Wang and Daniel M. Mittleman\*

Rice University, Department of Electrical and Computer Engineering, MS 366, Houston, Texas 77251-1892, USA

(Received 9 January 2006; published 17 April 2006)

We report the experimental and theoretical study of the dispersive behavior of surface plasmon polaritons (SPPs) on cylindrical metal surfaces in the terahertz frequency range. Time-domain measurements of terahertz SPPs propagating on metal wires reveal a unique structure that is inconsistent with a simple extrapolation of the high frequency portion of the dispersion diagram for SPPs on a planar metal surface, and also distinct from that of SPPs on metal nanowires observed at visible and near-infrared frequencies. The results are consistent with a numerical solution of Maxwell's equations, showing that the dispersive behavior of SPPs on a cylindrical metal surface at terahertz frequencies is quite different from that of SPPs on a flat surface. These findings indicate the increasing importance of skin effects for SPPs in the terahertz range, as well as the enhancement of such effects on curved surfaces.

DOI: 10.1103/PhysRevLett.96.157401

PACS numbers: 78.47.+p, 41.20.Jb, 73.20.Mf, 78.68.+m

Surface plasmon polaritons (SPPs) at metal-dielectric interfaces have been studied for several decades as a reliable technique for surface analysis and investigation of thin films [1]. Recently, SPPs have attracted special attention for their relevance in subwavelength optics and nanophotonics [2–4]. In particular, SPPs that are confined on metal nanowires are considered a promising alternative to dielectric waveguides in highly miniaturized integrated optical devices [4–9]. While most studies of SPPs focus on the visible and infrared frequency range, recent years have seen increasing interest in the study of SPPs in the terahertz (THz) frequency range, on both flat [10–13] and cylindrically shaped [14–16] surfaces. Because of the extremely low loss and low dispersion of SPPs in the THz frequency range, metal wire waveguides have received immediate attention for applications in THz imaging and spectroscopy [15–22].

For the development of plasmonic devices based on metal wire waveguides, a detailed knowledge of the SPP dynamics on cylindrical metal surfaces is essential. In this Letter, we report an experimental study of SPP dispersion on metal wires at THz frequencies. These data reveal the unusual dispersive behavior of SPPs on cylindrical metal surfaces in this frequency range. The observed results are different from the intuitive expectation of a simple extrapolation of the high frequency portion of the dispersion diagram of SPPs on a planar metal surface. For SPPs on a planar metal surface, the dispersion curve asymptotically approaches the light line  $k = \omega/c$  as the frequency decreases, and accordingly, the phase velocity and group velocity gradually increase and approach  $c$ , the speed of light in air [1]. Similar behavior has also been observed for SPPs propagating on Au and Ag nanowires at visible and near-infrared frequencies [6,8,9]. Our results indicate that SPPs on cylindrical metal surfaces show the opposite dispersive trend: the value of the phase velocity drops as the frequency decreases. This trend becomes increasingly evident as the diameter of the metal wire decreases.

Numerical solutions of Maxwell's equations give similar results and show that this phenomenon can only be observed in the low-frequency (i.e., THz) range, at frequencies far below that of the bulk plasma frequency. The observed deviation from the expected dispersion relation, although small, indicates an important mechanism which must be considered in the propagation of low-frequency SPPs: the combined action of skin effects and surface geometry.

We study the dispersive behavior of SPPs on cylindrical metal surfaces using terahertz time-domain spectroscopy (THz-TDS). This technique permits the coherent detection of the electric field of broadband SPP pulses with subpicosecond resolution, so that the dispersion relation of SPPs over a broad bandwidth can be easily reconstructed [23].

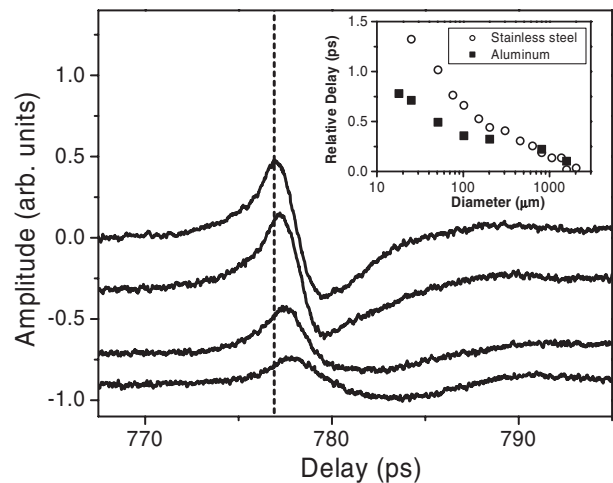


FIG. 1. (a) Time-domain waveforms of THz SPP pulses after propagating 20 cm on aluminum wires with diameters of 2388  $\mu\text{m}$ , 813  $\mu\text{m}$ , 51  $\mu\text{m}$ , and 18  $\mu\text{m}$  (from top to bottom). The inset shows the time delay of the peak of the detected THz waveforms relative to that of waveform measured on the largest wire, for both aluminum and stainless steel wires.

To investigate the effect of surface curvature, we measure the guided propagation of broadband THz pulses on stainless steel and aluminum wires, with diameters ranging from 2.4 mm down to 18  $\mu\text{m}$ . The experimental setup for the THz-TDS measurement is similar to that described in our earlier publications [15,20]. The metal wire is supported and stretched by a tightly fitting Teflon slab close to the distal end. The broadband single-cycle pulses of free space THz radiation are coupled to surface waves on the metal wire by scattering at a small ( $\sim 400 \mu\text{m}$ ) gap defined by the surface of the wire and a copper blade oriented perpendicular to the wire [13,15]. After a propagation distance of 20 cm, the electric field of the guided wave is detected by a fiber-coupled photoconductive antenna located 3 mm off the axis of the metal wire. For consistency with our earlier results, we have confirmed that the propagating wave is a radially polarized Sommerfeld wave by measuring the polarity reversal of the single-cycle THz pulse on opposite sides of the wire [15,20]. We compare a series of measurements using wires of different diameters, while all other components stay fixed.

The time-domain electric field waveforms detected on different Al wires are shown in Fig. 1(a). For clarity, only four typical waveforms are shown here. The detected THz pulses maintain the single-cycle shape, showing that the SPP propagation is largely nondispersive. That is, the dispersion relation is largely linear within the bandwidth of the detected radiation (from 30 GHz up to about 500 GHz). However, we observe an increase in the transit time as the diameter of the wire decreases, as shown in the inset of Fig. 1. Increased pulse reshaping becomes evident when the diameter is below 200  $\mu\text{m}$ . This indicates that the dispersion relation is no longer linear when the diameter of the metal wire waveguide becomes sufficiently small. The results for stainless steel are qualitatively similar, except that the increase in transit time is somewhat larger for a given wire diameter.

Detailed information concerning the propagation of the SPPs can be extracted from the Fourier transforms of the measured time-domain waveforms, which provide both the spectral amplitude and spectral phase [23]. From Fig. 1, it is clear that the amplitude of the SPP decreases with decreasing wire size. This is due both to a decrease in the input coupling efficiency as well as to increasing propagation losses on smaller wires. Of more interest is the spectral phase, from which we obtain the phase velocity  $v_p = L/\tau_p$ , where  $L$  is the propagation distance and  $\tau_p$  is the phase time delay. This delay is related to the measured spectral phase by

$$\tau_p(\omega) = \tau_0 + \frac{\Delta\phi(\omega)}{\omega} \quad (1)$$

where  $\tau_0$  is a reference phase time delay and  $\Delta\phi(\omega)$  is the phase difference between the detected waveform and the reference waveform. As shown below, for large wire diameters (e.g., larger than 1 mm), the SPP dispersion in the

THz range approaches that of a flat metal surface. The propagation is essentially dispersionless, and the velocity approaches the speed of light in air. Therefore, we use the THz waveform measured on the largest diameter wire (2.388 mm) as the reference pulse with  $\tau_0 = L/c$ . Here,  $c$  is the speed of light in air ( $c = c_0/\sqrt{\epsilon_{\text{air}}}$ ,  $c_0 = 2.9979 \times 10^8$  m/s,  $\epsilon_{\text{air}} = 1.0005364$  [24]). In Fig. 2 we plot the experimentally determined phase velocity  $v_p(\omega)$  for three different wire diameters. At all frequencies, the phase velocity decreases as the wire size decreases. This accounts for the increasing delay observed in Fig. 1. These data also show that, rather than approaching the speed of light  $c$ , the phase velocity deviates increasingly from  $c$  as the frequency decreases. This means that the low-frequency components arrive later than the peak of the pulse rather than earlier. This is distinct from the behavior of SPPs on a planar metal surface, which show the opposite trend albeit with a much smaller magnitude [1].

The theoretical study of electromagnetic surface modes on metal wires began as early as 1899 when Sommerfeld calculated the solution of Maxwell's equations for wave propagation along a cylindrical metal surface [25]. This type of surface wave, known as a Sommerfeld wave, has

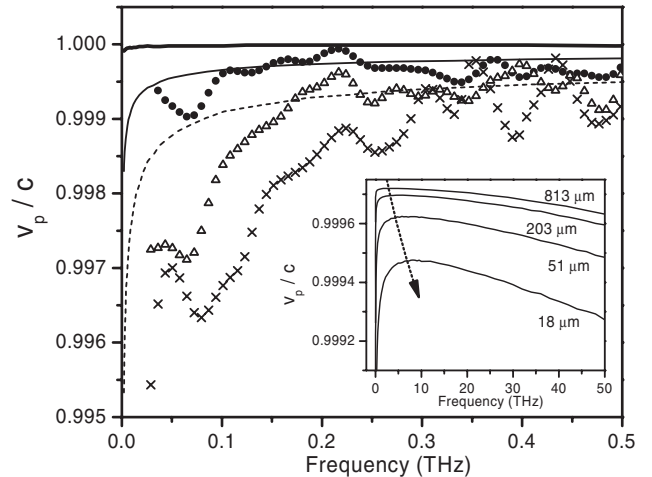


FIG. 2. The dots ( $\bullet$ ), triangles ( $\Delta$ ), and crosses ( $\times$ ) show the experimentally determined phase velocity of SPP's propagating on Al wires of diameters 813  $\mu\text{m}$ , 203  $\mu\text{m}$ , and 18  $\mu\text{m}$ , respectively (with the 2388  $\mu\text{m}$  wire used as a reference). The calculated phase velocities of these three wires (also referenced to the largest wire) are shown by the thick solid line, the thin solid line, and the dashed line, respectively. The weak oscillatory features in the data are not reproducible, and are due to noise in the measurements. The amplitude of these features is a rough indication of the error bars for these data points, as defined by the variation between successive measurements taken under identical conditions. The inset shows the calculated phase velocities over a broader spectral range, for four wire diameters as indicated. The turnover and rapid decrease of  $v_p$  at low frequencies is a unique feature of the curved surface; SPPs propagating on a flat surface do not exhibit this feature. As expected from the discussion given in the text, the turnover point moves to increasing frequency as the wire diameter decreases.

been studied from radio frequencies to millimeter waves [26–28]. However, there has been no systematic experimental characterization of the dispersion of these propagating surface waves. On the other hand, the study of SPPs on metal wires at optical frequencies first appeared in the 1970s [29–31], and has recently received considerable attention [4–9]. The latest theoretical and experimental studies have shown that the dispersive behavior of SPPs on Au and Ag nanowires is similar to that of a planar metal-dielectric interface at visible and near-infrared frequencies [6,8,9]. This is in contrast to what we observe in the THz frequency range, where the distinct behavior of the cylindrical geometry is more clearly revealed.

To understand the unusual dispersive behavior of SPPs on metal wires in the THz frequency range, we calculate the dispersion relation of SPPs over the whole frequency range from THz to visible light, for both a planar Al surface and Al wires with various diameters. The dispersion relation for a planar Al surface is given by Eq. (2.4) in Ref. [1]. Our direct measurement of the spatial profile of the guided electromagnetic mode on metal wires [15] has shown that the surface mode is the azimuthally symmetric zeroth-order transverse magnetic (TM) mode [25,26]. The dispersion relation of this mode can be obtained by numerically solving the transcendental equation [25]

$$\frac{k_{\text{Al}}^2}{\mu_{\text{Al}}\gamma_{\text{Al}}} \frac{J_1(\gamma_{\text{Al}}a)}{J_0(\gamma_{\text{Al}}a)} = \frac{k_{\text{air}}^2}{\mu_{\text{air}}\gamma_{\text{air}}} \frac{H_1^{(1)}(\gamma_{\text{air}}a)}{H_0^{(1)}(\gamma_{\text{air}}a)}. \quad (2)$$

Here  $a$  is the radius of the wire,  $\mu$  is the magnetic permeability,  $k$  is the propagation constant in a homogeneous medium,  $\gamma$  is defined as  $\gamma^2 = k^2 - h^2$ , and  $h$  is the propagation constant of the surface mode.  $J_0$  and  $J_1$  are Bessel functions;  $H_0^{(1)}$  and  $H_1^{(1)}$  are Hankel functions. We model the properties of aluminum using a Drude model, with the parameters taken from Refs. [24,32]. To make the calculation valid over a very broad frequency range, we do not use the low-frequency approximation  $k_{\text{Al}} = (\omega\mu_{\text{Al}}\sigma_{\text{Al}})^{1/2} \exp(-i\pi/4)$  or the high frequency approximation  $\varepsilon(\omega) = 1 - \omega_p^2/\omega^2$  as in previous work [16,26,28,31]. The only approximation used in our calculation is  $J_1/J_0 = -i$ , which is valid because the radius of the wires used here are large compared to the skin depth ( $|\gamma_{\text{Al}}a| \gg 1$ ) [26,28,33]. The calculated dispersion relation is shown in Fig. 3. At visible and infrared frequencies, the dispersive behavior of an SPP on an Al wire of 25  $\mu\text{m}$  diameter is almost indistinguishable from that of a planar Al surface. But as shown in the inset, the low-frequency portion of the dispersion curve approaches the light line in a different way from that of a planar surface, which leads to the unique dispersive behavior observed in the THz frequency range. For comparison with the experimental data, we calculate the phase velocity of the SPPs on Al wires of several different diameters. The results are shown as solid curves in Fig. 2. The calculated phase velocity agrees qualitatively with the observed results, reproducing, in

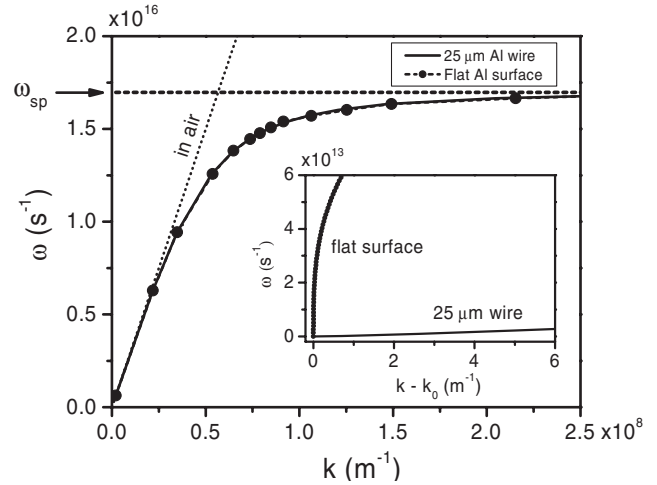


FIG. 3. Calculated dispersion relations for SPPs on a planar Al surface and on an Al wire of 25  $\mu\text{m}$  diameter, together with the plane wave dispersion relation in air.  $\omega_{\text{sp}}$  is the theoretical value of the surface plasmon frequency [35]. The inset shows a zoomed-in view of the low-frequency portion of the dispersion diagram. In this inset, we plot  $\omega$  against  $k - k_0$ , where  $k_0$  denotes the propagation constant of plane waves in air.

particular, the notable feature of the decreasing  $v_p$  with decreasing frequency. We obtain similar results for our measurements on stainless steel wires (not shown); the larger pulse delay shown in Fig. 1 (inset) is a result of the lower conductivity of stainless steel as compared to aluminum.

We note that, in Fig. 2, the observed departure of  $v_p$  from  $c$  is somewhat larger than the computed values, for all wire diameters. The origin of this discrepancy remains unclear; it may be due to the inadequacy of the Drude model in describing the dielectric properties of metals at THz frequencies [34].

When viewed over a broader frequency range (the inset of Fig. 2), it is clear that this unusual dispersive behavior only appears at THz and lower frequencies. This result indicates that for frequencies much lower than the surface plasmon frequency  $\omega_{\text{sp}}$  [35], the resonant interaction between the electromagnetic wave and the plasma oscillation is no longer the dominant mechanism for determining the properties of surface waves. The electromagnetic properties of the metal play an increasingly important role due to the larger skin depth at lower frequencies [36]. The electric field and current that penetrate into the metal change the surface impedance and the internal inductance, and therefore affect the dispersive behavior of the surface waves [37–39]. This effect is enhanced for SPPs propagating on wires, due to the geometry of the metal surface. Since Sommerfeld waves are single-mode azimuthally symmetric TM waves [15,25,26,38], the electric field components inside the metal at a given point along the length of the wire are in phase. So, due to the curved nature of the surface, these evanescent field components can constructively interfere inside the metal. As a result, more power is trans-

mitted inside the metal for SPPs on metal wires as compared to SPPs on planar metal surfaces. This enhanced skin effect is more significant for smaller wire diameters, since increased surface curvature leads to a larger overlap of the evanescent waves penetrating into the metal. It is also more significant at lower frequencies, due to the larger skin depth. This model is consistent with the simulations shown in the inset of Fig. 2, particularly the shift of the turning point of the  $\nu_p$  curves to higher frequencies as the wire diameter decreases.

In conclusion, we report the first systematic study of the dispersion of SPPs on cylindrical metal surfaces in the terahertz frequency range. The dispersion relation deviates from linearity, in a way that is different from that of SPPs on a planar metal surface, and also from that of SPPs on metal nanowires observed at visible and near-infrared frequencies. This behavior becomes increasingly evident with the decrease of the diameter of the wire, and can only be observed in the low-frequency regime, far below the bulk plasmon frequency. This unusual dispersive behavior indicates the decreased plasmonic nature of SPPs in the THz frequency range.

This work was supported in part by Advanced Micro Devices, by the R. A. Welch Foundation, and by the National Science Foundation.

---

\*To whom correspondences should be addressed.

Email address: daniel@rice.edu

Phone number: 713-348-5452

Fax number: 713-348-5686

- [1] H. Raether, *Plasmons on Smooth and Rough Surfaces and on Gratings* (Springer-Verlag, Berlin, 1988).
- [2] T. W. Ebbesen, H. J. Lezec, H. F. Ghaemi, T. Thio, and P. A. Wolff, *Nature (London)* **391**, 667 (1998).
- [3] J. B. Pendry, *Phys. Rev. Lett.* **85**, 3966 (2000).
- [4] W. L. Barnes, A. Dereux, and T. W. Ebbesen, *Nature (London)* **424**, 824 (2003).
- [5] R. M. Dickson and L. A. Lyon, *J. Phys. Chem. B* **104**, 6095 (2000).
- [6] G. Schider, J. R. Krenn, A. Hohenau, H. Ditlbacher, A. Leitner, F. R. Aussenegg, W. L. Schaich, I. Puscasu, B. Monacelli, and G. Boreman, *Phys. Rev. B* **68**, 155427 (2003).
- [7] M. I. Stockman, *Phys. Rev. Lett.* **93**, 137404 (2004).
- [8] J.-C. Weeber, Y. Lacroute, A. Dereux, E. Devaux, T. Ebbesen, C. Girard, M. U. González, and A.-L. Baudrion, *Phys. Rev. B* **70**, 235406 (2004).
- [9] J. K. Lim, K. Imura, T. Nagahara, S. K. Kim, and H. Okamoto, *Chem. Phys. Lett.* **412**, 41 (2005).
- [10] D. Qu, D. Grischkowsky, and W. Zhang, *Opt. Lett.* **29**, 896 (2004).
- [11] J. F. O'Hara, R. D. Averitt, and A. J. Taylor, *Opt. Express* **12**, 6397 (2004).
- [12] H. Cao and A. Nahata, *Opt. Express* **12**, 1004 (2004).
- [13] J. Saxler, J. Gómez Rivas, C. Janke, H. P. M. Pellemans, P. Haring Bolivar, and H. Kurz, *Phys. Rev. B* **69**, 155427 (2004).
- [14] K. Wang, A. Barkan, and D. M. Mittleman, *Appl. Phys. Lett.* **84**, 305 (2004).
- [15] K. Wang and D. M. Mittleman, *Nature (London)* **432**, 376 (2004).
- [16] T.-I. Jeon, J. Zhang, and D. Grischkowsky, *Appl. Phys. Lett.* **86**, 161904 (2005).
- [17] Q. Cao and J. Jahns, *Opt. Express* **13**, 511 (2005).
- [18] H. Cao and A. Nahata, *Opt. Express* **13**, 7028 (2005).
- [19] N. C. J. van der Valk and P. C. M. Planken, *Appl. Phys. Lett.* **87**, 071106 (2005).
- [20] K. Wang and D. M. Mittleman, *J. Opt. Soc. Am. B* **22**, 2001 (2005).
- [21] M. Wächter, M. Nagel, and H. Kurz, *Opt. Express* **13**, 10 815 (2005).
- [22] M. Walthers, M. R. Freeman, and F. A. Hegmann, *Appl. Phys. Lett.* **87**, 261107 (2005).
- [23] D. Mittleman, *Sensing with Terahertz Radiation* (Springer-Verlag, Heidelberg, 2002).
- [24] D. R. Lide, *CRC Handbook of Chemistry and Physics* (CRC Press, Boca Raton, 2004).
- [25] J. A. Stratton, *Electromagnetic Theory* (McGraw-Hill, New York, 1941).
- [26] G. Goubau, *J. Appl. Phys.* **21**, 1119 (1950).
- [27] F. Sobel, F. L. Wentworth, and J. C. Wiltse, *IRE Trans. Microwave Theor. Tech.* **9**, 512 (1961).
- [28] M. J. King and J. C. Wiltse, *IRE Trans. Antennas Propagation* **10**, 246 (1962).
- [29] C. Miziumski, *Phys. Lett. A* **40**, 187 (1972).
- [30] J. C. Ashley and L. C. Emerson, *Surf. Sci.* **41**, 615 (1974).
- [31] C. A. Pfeiffer, E. N. Economou, and K. L. Ngai, *Phys. Rev. B* **10**, 3038 (1974).
- [32] N. W. Ashcroft and N. D. Mermin, *Solid State Physics* (Saunders College, Philadelphia, 1976).
- [33] The value of  $|\gamma_{Al}a|$  increases with both frequency  $f$  and radius  $a$ . Our calculation shows that the minimum value is  $|\gamma_{Al}a| \approx 22.6$  for  $f = 20$  GHz and  $a = 18 \mu\text{m}$ . So the assumption  $|\gamma_{Al}a| \gg 1$  is valid for all frequencies and wire diameters discussed in this paper.
- [34] T.-I. Jeon and D. Grischkowsky, *Phys. Rev. Lett.* **78**, 1106 (1997).
- [35] The surface plasmon frequency  $\omega_{sp}$  is determined by  $\omega_{sp} = \omega_p / \sqrt{\epsilon_{air} + 1}$  where  $\omega_p$  is the bulk plasma frequency of Al.
- [36] J. D. Jackson, *Classical Electrodynamics* (John Wiley & Sons, New York, 1975).
- [37] H. A. Wheeler, *Proc. IRE* **30**, 412 (1942).
- [38] H. M. Barlow and A. L. Cullen, *Proc. Inst. Electr. Eng.* **100**, 329 (1953).
- [39] W. Heinrich, *IEEE Trans. Microwave Theory Tech.* **38**, 1468 (1990).